Received: 21 December 2020 | Revised: 27 August 2021 | Accepted: 1 September 2021

DOI: 10.1111/geb.13407

Global Ecology and Biogeography | A Journal of Macroecology

WILEY

RESEARCH ARTICLE

Disturbance frequency, intensity and forest structure modulate cyclone-induced changes in mangrove forest canopy cover

Jonathan Peereman[1] | J. Aaron Hogan[2] | Teng-Chiu Lin[1]

[1]Department of Life Science, National Taiwan Normal University, Taipei, Taiwan

[2]Department of Biological Sciences, Florida International University, Miami, Florida, USA

Correspondence
Teng-Chiu Lin, Department of Life Science, National Taiwan Normal University, Taipei 11677, Taiwan.
Email: tclin@ntnu.edu.tw

Funding information
Ministry of Science and Technology grant number: MOST 107-2313-B-003-001-MY3

Handling Editor: Sean Michaletz

Abstract

Aim: Tropical cyclones are large-scale disturbances that can shape the structure and dynamics of mangrove forests. Although tropical cyclone activity overlaps extensively with the latitudinal distribution of mangrove forests, the relationships between cyclone intensity and frequency and mangrove forest canopy damage and recovery are not understood at the global scale. Using remote sensing data, we examined how mangrove forest structure, climate and cyclone characteristics influence canopy cover loss and recovery dynamics.

Location: Global tropics.

Time period: 2000–2020.

Major taxa studied: Mangrove trees.

Methods: Using two satellite-derived vegetation indices (the enhanced vegetation index and the normalized difference infrared index) from 86 cyclones affecting 56 mangrove sites across the globe, we quantified mangrove canopy loss in relationship to cyclones. Using linear regression and variance decomposition, we identified and ranked significant predictors of cyclone-induced canopy loss and recovery.

Results: Three-quarters of the studied cyclone disturbances resulted in canopy damage. Stands exposed to high wind speeds and those close to the cyclone paths were more severely damaged, whereas lower damage magnitudes were found in sites with greater past cyclone frequency. Canopy damage was greater in tall mangrove stands but decreased with higher aboveground biomass. The distance from the cyclone path and maximum wind speed were the most important factors, representing > 50% of the explained variation in cyclone damage. There was considerable variation in canopy damage among cyclones, but rates of recovery were similar across all mangrove sites, with the main predictor of recovery time being the degree of canopy loss.

Main conclusions: Our results suggest that the resistance of mangrove canopy cover to cyclone disturbance is variably tuned to the cyclone regime and vegetation characteristics, but resilience is inherent to the magnitude of canopy damage because the rate of forest canopy recovery appears to be consistent globally.

KEYWORDS

canopy cover, disturbance, enhanced vegetation index, forest structure, mangroves, normalized difference infrared index, remote sensing, resilience, tropical cyclones

1 | INTRODUCTION

Globally, mangrove forests are facing many threats, including timber harvest (Din et al., 2008), sea-level rise (Lovelock et al., 2015) and shifts in rainfall, temperature and disturbance drivers because of climate change (Alongi, 2015). Among these threats, climate change-induced changes in tropical cyclone disturbance regimes are unique because of the global distribution of mangrove forests, which largely overlaps with the extent of tropical cyclone activity (Figure 1). Mangrove forests are situated at the terrestrial–marine ecotone and are therefore particularly prone to the high winds, heavy rains and storm surge of cyclones. The projected increase in the frequency of the most intense cyclones (Kossin et al., 2020), coupled with their projected coastal migration (Wang & Toumi, 2021), is likely to alter significantly and, potentially, to accelerate mangrove forest dynamics in the coming decades. Studies on the response and recovery of mangrove forests experiencing cyclones of different frequencies and intensities at the global scale are rare (but see Simard et al., 2019a), but they have potential to help us to understand how changing cyclonic storm regimes will affect mangrove forests.

The strong winds, heavy rains and large tidal surges of cyclones can disturb mangroves directly by damaging trees and modifying the environment (Krauss & Osland, 2020), often more so than for terrestrial forests. Through defoliation, branch breaking and tree windthrow (Doyle et al., 1995; Smith et al., 1994), cyclones influence forest structure (i.e., tree height and stem size distributions) and cause canopy dwarfing (Lin et al., 2020) because taller, more exposed trees are removed disproportionally by cyclones (Doyle et al., 1995; Smith et al., 1994). Furthermore, disturbance-driven environmental changes, such as soil deposition (Castañeda-Moya et al., 2020), erosion, hydrological changes and increasing temperature because of canopy loss, stress mangroves (Doyle et al., 1995; Radabaugh et al., 2020). For example, mangrove dieback across the Everglades landscape of coastal South Florida in relationship to Hurricane Irma was attributable to storm surge water ponding and hydrological isolation and not directly to wind (Lagomasino et al., 2021). Cyclones also influence mangrove ecosystem carbon cycling via effects on forest primary productivity, litterfall and necromass generation (Adame et al., 2013; Castañeda-Moya et al., 2013). Given that cyclone disturbance events cause canopy damage, which leads to lower canopy CO_2 assimilation rates (Barr et al., 2012), thorough studies of mangrove forest canopy loss and recovery dynamics are important for understanding and modelling the carbon balance in cyclone-affected landscapes where mangrove forests represent large carbon stocks (Cameron et al., 2021).

Variation in disturbance frequency might explain regional differences in mangrove forest structure and dynamics (Rovai et al., 2016; Simard et al., 2019a). For instance, the tallest mangroves in the world are found in areas unaffected by cyclones (e.g., the Gabon Estuary and other cyclone-free equatorial regions; Simard et al., 2019a), probably because they lack the canopy-dwarfing effects of cyclones (Lin et al., 2020). On the contrary, mangroves are short on Yap island, Micronesia because of frequent cyclones (Allen et al., 2000). Moreover, a remote sensing-based study of the 2017 hurricane season in the Caribbean identified recent hurricane history as a significant factor explaining variation in forest normalized difference vegetation index (NDVI) response (i.e., resilience) to cyclone disturbance (Taillie et al., 2020). Forests repeatedly exposed to

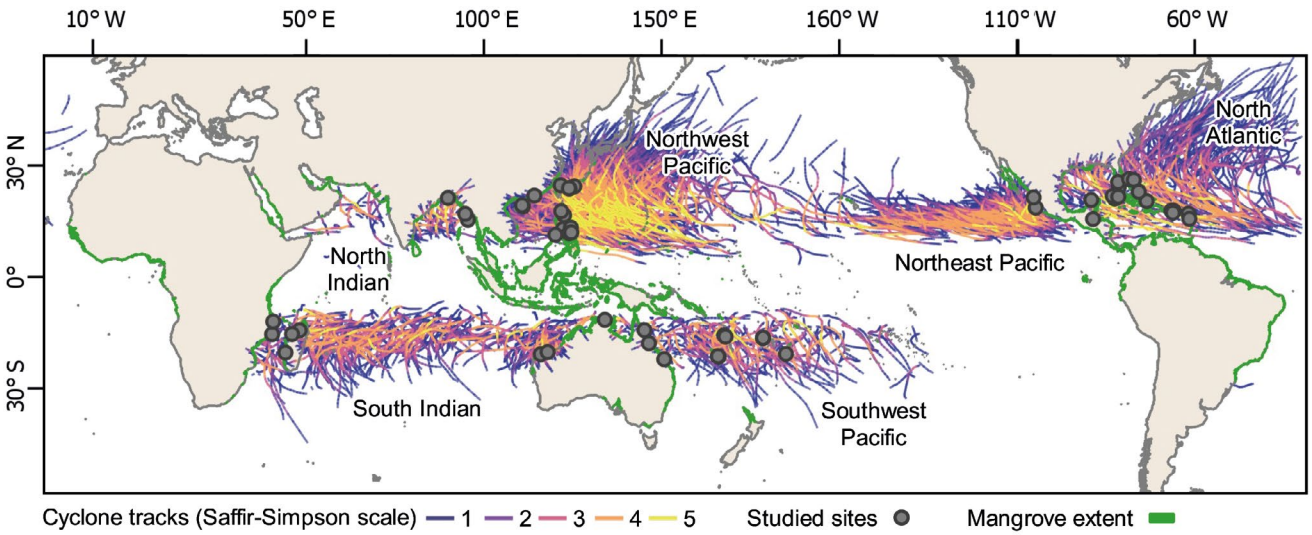

FIGURE 1 Cyclone tracks, locations (grey dots) of studied mangrove forests ($n = 56$) and global mangrove distribution. Cyclone tracks are colour coded by storm intensity for all storms of at least category 1 on the Saffir–Simpson scale since 1980 based on the International Best Track Archive for Climate Stewardship (IBTrACS) archive (Knapp et al., 2010, 2018). Mangrove distribution, shown in green, is based on the Global Distribution of Mangroves dataset (Giri et al., 2011). The Supporting Information (Table S1) gives further information about each studied mangrove forest. Detailed maps of each studied mangrove forest in relationship to cyclone paths are shown in the Supporting Information (Figures S1–S6)

high winds have high resistance to disturbance because the gradual removal of taller and therefore more exposed trees or branches leads to short and homogeneous canopies that are more resistant to wind forces (Krauss & Osland, 2020; Lin et al., 2020; Roth, 1992). Although Simard et al. (2019a) have examined the relationship between mangrove structure and cyclone frequency, no assessments on the effects of the frequency or strength of cyclones on mangrove forest canopy cover dynamics have been carried out at the global scale. This hinders our understanding of mangrove forest resilience, or the ability of mangroves to sustain disturbance and recover to the pre-disturbance structural state (Holling, 1973), in relationship to cyclones, a key driver of disturbance that is projected to increase in importance with climate change.

Owing to the global variation in the frequency of cyclones, a selection of sites from all cyclone basins allows one to test whether mangrove forests in sites with more frequent cyclones are less affected by, and recover more rapidly from, cyclone disturbance. Such a global scope would also include mangrove forests with very different forest structures and climate characteristics and therefore allow for evaluation of how forest structure and climate influence the response of mangrove forests to cyclone disturbances. Using vegetation indices (VIs) derived from time series satellite images of mangrove forests from across the world, we questioned:

1. What is the role and relative importance of variables related to cyclone, vegetation and climatic characteristics on the variation of cyclone damage?
2. How does cyclone frequency relate to cyclone-induced changes in mangrove forest canopy cover?
3. Do more frequently disturbed mangroves recover to their pre-cyclone VI values more rapidly than less frequently disturbed ones?
4. Is mangrove forest structure [i.e., aboveground biomass (AGB) and canopy height] related to cyclone-induced variation of VIs and their post-cyclone recovery?

2 | MATERIALS AND METHODS

2.1 | Site and cyclone selection

Our site selection was based on four criteria: (1) a close distance (< 100 km) to at least one major cyclone; (2) available cloud-free remote sensing imagery; (3) minimal anthropogenic influence; and (4) being representative of the relative frequency of cyclones among the six cyclone basins. We defined major cyclone events as storms of at least category 3 (wind speeds > 178 km/h; Simpson & Riehl, 1981) between 2000 and 2020, using the International Best Track Archive for Climate Stewardship (IBTrACS) archive (Knapp et al., 2010, 2018). Storms of at least category 3 typically result in significant and more noticeable forest damage (Kauffman & Cole, 2010) and litterfall than category 1 and 2 cyclones (Lin et al., 2003). Additionally, the number of cyclones of at least category 3 is projected to increase in the coming decades as climate change intensifies (Kossin et al., 2020).

To minimize the confounding effects of anthropogenic disturbances, most sites (43 of 56) were selected within nature reserves, although this classification was limited by the data available in the World Database of Protected Areas (UNEP-WCMC, 2020). Given that mangrove forest fragments are more likely to experience anthropogenic pressures that might confound or modulate the effects of cyclones (Branoff, 2017), the 13 other sites were selected because they represented unfragmented patches (i.e., pixels grouped together rather than separated by non-vegetated gaps) within the Global Distribution of Mangroves dataset (based on visual inspection; Giri et al., 2011). Globally, although many mangroves were within 100 km of major cyclones, site selection was largely limited by the availability of cloud-free pre- and post-cyclone satellite images and by the Scan Line Corrector failure of Landsat 7. By selecting unfragmented sites with unknown levels of protection, we increased the number of events and improved the representation of events from basins of lower cyclone activity (e.g., the southern and northern Indian Ocean basins). Based on the above considerations, we selected 56 mangrove forest sites across all cyclone basins (Figure 1; Supporting Information Table S1). Although the 56 mangrove forests were selected based on the occurrence of at least one cyclone of at least category 3, once a site was selected we studied the effects of all cyclones of at least category 1 on the Saffir–Simpson scale (i.e., those with wind speeds > 119 km/h) on VI if pre- and post-cyclone cloud-free images were available. As a result, a total of 64 cyclones affecting the 56 sites were analysed, with 12 cyclones affecting more than one site and therefore being analysed for multiple sites. Thus, if the effect of one cyclone on one site is considered as a single disturbance event, the dataset includes 86 events. Site locations (Figure 1), storm meteorological details (Supporting Information Table S1) and the paths of selected cyclones are detailed in the Supporting Information (Figures S1–S6).

2.2 | Remotely sensed data processing

Scenes (i.e., imagery) derived from 30-m spatial resolution Landsat Thematic Mapper (TM), Enhanced Thematic Mapper (ETM+) and Operational Land Imager (OLI) sensors, processed to surface reflectance and then to VIs, were downloaded from the USGS EarthExplorer website (earthexplorer.usgs.gov; as listed in Supporting Information Table S2). We removed surfaces obscured by clouds and cloud shadows within each scene using the pixel quality assessment band that is provided with each scene by the USGS. No topographic correction was applied because mangrove environments have relatively flat topography.

We used the enhanced vegetation index (EVI; Huete et al., 2002) and the normalized difference infrared index (NDII; Hardisky et al., 1983) to follow the extent of mangrove vegetation cover. The EVI, a VI based on blue, red and near-infrared (NIR) wavelengths, is

more sensitive overall to variation in canopy reflectance at high levels of vegetation biomass than the commonly used normalized difference vegetation index (Huete et al., 1997). The NDII is based on the NIR and short-wave infrared (SWIR) bands and is highly sensitive to leaf chlorophyll and water content (Cheng et al., 2006). Both indices have been shown to be good remotely sensed metrics of changes in forest canopy cover and canopy leaf physiology associated with cyclones, including mangroves, although they are limited by their sensitivity to light canopy damage (Peereman et al., 2020; Zhang et al., 2016). Moreover, the SWIR band and the NDII have been used successfully to follow mangrove recovery (Gang et al., 2020; Peneva-Reed et al., 2020). We calculated cyclone-induced absolute change in a VI ($\Delta VI_{absolute}$), or the difference between pre-cyclone and post-cyclone VI values, and the relative VI change ($\Delta VI_{relative}$), or the ratio of absolute change to the pre-cyclone value, represented as a percentage.

All scenes were acquired within 1–2 months before and after cyclone passage, which minimizes the effect of early recovery and leaf turnover (Pastor-Guzman et al., 2018). We also acquired images preceding and following each cyclone event for ≤ 9 years to assess mangrove recovery. We assumed that a site had recovered when its VI was not different from the VI measured before disturbance (≤ 2 years before, accounting for inter-annual variability in the absence of other cyclones). Therefore, when data were available, we added annual scenes until we could detect VI recovery. For each site, we compared scenes that were acquired during the same season to reduce the effect of phenological change in the forest canopy across years. The dates of images across years were at most a few weeks apart.

2.3 | Data on forest stands structure and climate

For each of the 56 mangrove sites, two measures of forest structure, AGB (in megagrams per hectare) and forest canopy height (mean maximum height, in metres), were acquired from the dataset for the year 2000 provided by Simard et al. (2019b) for world-wide mangroves with a 30 m spatial resolution. The area of each study site was delimited with one shapefile by combining the Landsat pixel quality assessment bands and two world-wide mangrove distribution datasets: the Global Distribution of Mangroves and the Global Mangrove Watch data (GMW) from 1996 to 2016 (Bunting et al., 2018). The GMW helped to select mangrove surfaces that did not show land-use change between 1996 and 2016. To describe stand growth conditions, we extracted four climatic parameters from the WorldClim 2 dataset (Fick & Hijmans, 2017): mean annual temperature (in degrees Celsius), annual temperature range (monthly maximum–monthly minimum), total annual precipitation (in millimetres) and precipitation seasonality (i.e., the coefficient of variation of the annual precipitation). Pixel values were extracted from each image using R v.3.6.1 (R Core Team, 2019) and the "raster" package (Hijmans, 2019). For each site, only pixels common across all scenes used were analysed (i.e., never occulted by clouds or their shadows).

2.4 | Detection of change and correlations of cyclone parameters, forest structure and environment

Within each site, VI values were compared between all dates between 2000 and 2020 using the procedure described by Herberich et al. (2010) to detect the direction of VI change after cyclone passage and to monitor recovery dynamics across the following years. This procedure compares groups in the absence of a normal distribution and with heterogeneous variances, using the R packages "multicomp" and "sandwich" (Hothorn et al., 2008; Zeileis et al., 2020). The resulting 95% confidence intervals (95% CI) were used to assess whether cyclones led to a significant reduction in VI (i.e., $VI_{post\text{-}cyclone} < VI_{pre\text{-}cyclone}$, hereafter referred to as "damage") and when vegetation recovery occurred (i.e., when $VI_{post\text{-}cyclone\ n\ year} \geq VI_{pre\text{-}cyclone\ year}$). If the 95% CI of the mean difference between pre-cyclone and post-cyclone values encompasses zero, there is no significant difference between the pre- and post-cyclone VIs.

Spearman's correlation (ρ) was used to test whether the two VIs captured similar patterns of vegetation reduction for all sites and across all disturbance events. We also used Spearman's ρ to examine the relationships between wind speed and cyclone frequency and between mean AGB, mean maximum canopy height and cyclone frequency.

2.5 | Model selection

2.5.1 | Cyclone-induced change in relationship to forest, cyclone and climatic variables

All cyclone events from 2000 to 2020 were included when carrying out linear model selection, but ΔVIs were set to zero for cyclones that did not cause a decline in VIs. This was done because cyclones are unlikely to cause immediate positive change in VIs, meaning that the negative ΔVI values were unrelated to cyclones. Exploration of the methodological causes of VI increase is beyond the scope of this study. By setting the negative ΔVIs to zero, damaging cyclones were represented by $\Delta VI > 0$ and other events by zero. We standardized all independent variables (i.e., centred them on a mean of zero and scaled them to a standard deviation of one) and computed variance inflation factors (VIFs) to detect significant collinearities within sets of predictors. Predictors with a VIF ≥ 5 were excluded iteratively, starting with the predictor with the highest VIF, until no VIF remained above this threshold.

We modelled absolute and relative ΔVIs using standardized explanatory variables related to cyclone characteristics, forest structural properties and climate variables as predictors in ordinary least-squared multiple regression models. We ran stepwise backward model selection based on the Akaike information criterion (AIC) to select the best-fitting linear regression models. In addition to AIC, we report the difference in AIC along stepwise model selection (ΔAIC), Akaike weights (w_i) and the VIF scores of selected predictors. Moreover, we ranked explanatory variables using the

Lindeman, Merenda and Gold (LMG) method for variance decomposition from the "relaimpo" package (Grömping, 2006; Lindeman et al., 1980). The LMG values quantify the proportion of variance explained by each predictor in the multiple linear regression and range from zero to r^2 (i.e., LMG values can be interpreted as r^2 values for individual predictor variables), with the sum of LMG values equal to the model r^2.

Cyclone intensity and distance variables were derived from the IBTrACS database. Cyclone intensity was represented in the linear models using data of maximum sustained wind speed, defined in the IBTrACS database as the maximum value of the 10-min average wind speed within a 100 km range of the site centroid (in kilometres per hour; Knapp et al., 2018). Cyclone distance was represented in the linear models as the shortest distance between the cyclone path and the centroid of the site (in kilometres). Lastly, cyclone frequency was included in the linear models, as the number of named cyclones (i.e., at least category 1) that passed within 100 km of the site centroid between 1980 and 2020.

Variables related to vegetation cover and structural properties included pre-cyclone mean EVI or NDII, AGB and mean maximum canopy height (see section 2.3) because pre-disturbance forest structure and composition and total biomass are important factors in determining the magnitude of disturbance effects (Gough et al., 2021; Hogan et al., 2018; Kosugi et al., 2016; Lin et al., 2020). Although AGB and canopy height are likely to be correlated, we included both as predictors in the linear models. Canopy height is closely related to wind exposure, whereas AGB reflects forest structural attributes, such as average stem diameter at breast height (d.b.h.), and forest successional status, including tree densities, which also affect the vulnerability of mangroves to cyclone disturbance. Lastly, we included the four climatic variables described earlier (see section 2.3), mean annual temperature, annual temperature range, total precipitation and precipitation seasonality as predictors in the linear regression model selection.

2.5.2 | Analysis of mangrove forest canopy recovery from cyclone disturbance

Mangrove forest canopy recovery was studied for cyclones that caused a significant reduction in EVI or NDII in the month after the cyclone and if at least one image per year (at the same season) was available to monitor VI recovery (44 events). The time until canopy recovery (in years) was estimated by comparing VI measurements 1 or 2 years before cyclone passage and VI measured in the years after the cyclone. Given the slight but significant inter-annual variation in EVI and NDII (even without cyclone events), a mangrove stand was considered to have recovered if the VI value was greater than or equal to its pre-cyclone value. To account for small variation in VI values across years unrelated to cyclone disturbance, we considered that a mangrove stand had recovered if its VI value was greater than or equal to the value observed before the cyclone or within 2 years before if there were no other cyclones during that period. Incomplete VI recoveries by 2020 were not included in the analysis. The time to recovery between the two VIs was assessed with Spearman's ρ.

As in Section 2.5.1, we used stepwise backward model selection to select the best-fitting linear models that explained variation in the time to recovery of EVI and NDII. We included multiple standardized explanatory variables with VIFs < 5 in the model selection. First, we chose parameters describing the pre-disturbance state of the mangroves (pre-cyclone VI) and VI reduction (absolute and relative ΔVIs as proxies for damage severity) because severe damage can slow down recovery by limiting lateral canopy growth or propagule availability (Ferwerda et al., 2007; Radabaugh et al., 2020). In addition, immediate post-cyclone VI was included because it describes the post-disturbance state of the mangrove from which recovery begins. The following predictors that were used in our model selection for predicting VI reduction were also included in the model selection for VI recovery: mean maximum tree height, mean AGB, cyclone wind speed and frequency, in addition to the four climatic variables listed earlier.

3 | RESULTS

3.1 | Cyclone characteristics and induced changes in VI

We observed the effects of 13 category 1, seven category 2, 20 category 3, 25 category 4 and 21 category 5 cyclones from 2000 to 2020 on mangrove canopy-related VI values. Cyclone paths varied in their distance to selected mangrove forest sites, ranging from 2 to 99 km. The number of cyclones of at least category 1 affecting each site since 1980 varied from one (several sites) to 39 (Shimajiri forest in Japan, site 22). Sites that experienced the greatest frequency of cyclones were all located in the Northwest Pacific basin (Supporting Information Table S1). Interestingly, there was no significant correlation between cyclone frequency and the maximum sustained wind speed ($\rho = -.17$, $p = .11$, $n = 86$).

Cyclone disturbance induced a decrease in either EVI or NDII for 68 of 86 events and for 52 of the 56 studied sites (95% CIs are given in Supporting Information Table S3). Moreover, 47 events led to a significant decrease in both EVI and NDII. The most severe mangrove canopy damage was observed in Atlantic Mexico after Hurricane Isidore (category 3, site 51), which resulted in a reduction in absolute EVI of 0.36 (which is a 72% reduction for relative EVI) and a reduction of 0.51 in absolute NDII. Additionally, Cyclone Monica (a category 5 storm), which passed over Junction Bay in Australia (site 5), led to the most drastic relative reduction in NDII (121%; Supporting Information Table S3), probably because the soil was exposed and dry. Although the two ΔVIs disagreed on the occurrence of cyclone-induced vegetation loss for 18 cyclones (Supporting Information Table S3), their correlation was strong across all disturbance events (mean absolute and relative ΔEVI and ΔNDII, $\rho = .80$ and .80, $p < .01$, $n = 86$; Supporting Information Figure S7), showing

that they generally tracked similar changes in mangrove canopy cover properties.

3.2 | Relationships between ΔVIs and cyclone characteristics

The linear models indicated that distance and maximum wind speed significantly explained variation in absolute and relative ΔEVI and ΔNDII, whereas cyclone frequency was significant only for ΔEVI (Table 1 and Figure 2). Cyclone wind speed and distance contributed to more than half of the model-explained variance of ΔVIs according to the LMG method (28%–45% for distance and 24%–32% for wind speed; Figure 3), whereas the contribution of cyclone frequency was more moderate (11%–14%). The stepwise model selection progression and accompanying statistics for each model are summarized in the Supporting Information (Tables S4 and S5).

The magnitude of canopy damage, as measured by the change in VI values, increased significantly with increasing maximum sustained wind speed ($\Delta EVI_{absolute}$, $\beta = 0.03 \pm 0.01$; $\Delta EVI_{relative}$, $\beta = 5.98 \pm 1.67$; $\Delta NDII_{absolute}$, $\beta = 0.04 \pm 0.01$; $\Delta NDII_{relative}$, $\beta = 8.39 \pm 2.50$). Conversely, the magnitude of canopy damage decreased with increasing cyclone distance for both ΔEVI and ΔNDII ($\Delta EVI_{absolute}$, $\beta = -0.03 \pm 0.01$; $\Delta EVI_{relative}$, $\beta = -7.25 \pm 1.62$; $\Delta NDII_{absolute}$, $\beta = -0.05 \pm 0.01$; $\Delta NDII_{relative}$, $\beta = -10.70 \pm 2.45$). Changes of EVI were slightly smaller in sites with greater historical cyclone frequency ($\Delta EVI_{absolute}$, $\beta = -0.02 \pm 0.01$; $\Delta EVI_{absolute}$, $\beta = -3.97 \pm 1.84$; Table 1). In contrast, the ΔNDII-based models did not identify a significant relationship between damage severity and cyclone history ($p > .05$).

3.3 | Effect of biological and climatic characteristics on cyclone-induced vegetation changes

Pre-cyclone VIs contributed 2%–11% to the linear model fits (Figure 3). Mean AGB contributed 13%–20% to linear model fits, and mean maximum height contributed between 2% and 6%. The annual temperature range was the least important contributor of the linear model-explained variance for $\Delta EVI_{absolute}$ (3.70% of the model r^2) and was not included in the best-fitting model for ΔNDII.

Mean maximum canopy height had a significant correlation with AGB ($\rho = .60$, $p < .01$, $n = 56$), but neither maximum canopy height nor AGB was significantly correlated with cyclone frequency (p-values > .05, $n = 56$). Based on the coefficients from the linear models, stands with higher pre-cyclone EVI suffered more severe canopy damage ($\Delta EVI_{absolute}$, $\beta = 0.03 \pm 0.01$ and $\Delta EVI_{relative}$, $\beta = 4.07 \pm 1.85$; Table 1). On the contrary, stands with higher pre-cyclone NDII were less severely damaged ($\Delta NDII_{relative}$, $\beta = -5.55 \pm 2.36$). Although there was less damage to mangrove canopies with higher mean AGB ($\Delta EVI_{absolute}$, $\beta = -0.04 \pm 0.01$; $\Delta EVI_{relative}$, $\beta = -9.85 \pm 2.48$; $\Delta NDII_{absolute}$, $\beta = -0.05 \pm 0.02$; $\Delta NDII_{relative}$, $\beta = -9.63 \pm 3.73$; Table 1), damage increased for taller canopies ($\Delta EVI_{absolute}$, $\beta = 0.03 \pm 0.01$; $\Delta EVI_{relative}$, $\beta = 5.81 \pm 2.36$; $\Delta NDII_{absolute}$, $\beta = 0.03 \pm 0.02$). Among the selected predictors, mean AGB and mean maximum height had the greatest VIFs, but the values were below five, a key threshold for the measure of multicollinearity among variables (VIF ≤ 2.61; Supporting Information Table S4). Finally, annual temperature range was the only climatic variable selected, with wider temperature ranges being associated with greater reductions in $\Delta EVI_{absolute}$ ($\beta = 0.01 \pm 0.01$).

3.4 | Recovery of mangrove canopy vegetation after cyclone disturbance

The time to recovery of the two VIs (EVI and NDII) was strongly correlated ($\rho = .75$, $p < .01$, $n = 22$). Vegetation indices generally recovered within a few years, although there was considerable variation among and within study sites (Supporting Information Table S3). Rapid recovery, within 1 year for both VIs, was observed in multiple sites, such as in Australian mangroves (site 7) following Cyclone Christine (category 3) and in the Shimajiri Mangrove Forest of Japan (site 22) following Typhoon Lekima (category 4). Much slower recovery, which maximized at 9 years, was observed in a mangrove forest of Atlantic Mexico (site 51) following Hurricane Isidore (category 3), whereas complete recovery by 2020 could not be observed for seven studied cyclone events, with recovery times ranging from 2+ to 9+ years (Supporting Information Table S3).

Unlike cyclone-induced vegetation damage, cyclone characteristics (wind speed and distance) and vegetation characteristics (AGB or mean canopy height) did not help to explain the observed variation in canopy recovery times. These variables dropped out during model selection (Supporting Information Tables S4 and S5). The recovery time of EVI was significantly greater for sites with greater relative reduction in EVI ($\beta = 1.62 \pm 0.36$, 73% contribution of r^2; Table 2). Likewise, NDII recovery time was significantly longer for mangroves that experienced greater cyclone-induced declines in NDII ($\beta = 1.38 \pm 0.25$).

4 | DISCUSSION

4.1 | Cyclone damage to mangrove canopies depends on storm characteristics, forest structure and climate

The distance between the cyclone path and mangrove forests has long been understood to be a major factor influencing the magnitude of damage in single-region studies (e.g., Barr et al., 2012; Doyle et al., 1995). Direct cyclone passage (i.e., forest in the landfall site) causes severe damage to forest canopies (Zhang et al., 2019), and the severity of forest damage decreases with increasing distance from the path of the cyclone eye (Doyle et al., 1995; Smith et al., 1994). In accordance with single-region studies, we found that, at the global scale, closer cyclones induced greater canopy loss (i.e., vegetation

TABLE 1 Multiple linear regression coefficients [mean (*SE*)] and *t*-statistics with associated probabilities (*p*) for changes of absolute ($\Delta VI_{absolute}$) and relative ($\Delta VI_{relative}$) values of the enhanced vegetation index (EVI) and normalized difference infrared index (NDII) following cyclone disturbance

	$\Delta VI_{absolute}$				$\Delta VI_{relative}$			
Predictor	**Coefficient (*SE*)**	***t***	***p*-value**	**Partial r^2**	**Coefficient (*SE*)**	***t***	***p*-value**	**Partial r^2**
EVI								
Intercept	0.07 (0.01)	11.91	***	–	17.89 (1.52)	11.74	***	–
Wind speed	0.03 (0.01)	3.74	***	.15	5.98 (1.67)	3.59	***	.14
Distance	−0.03 (0.01)	−4.80	***	.23	−7.25 (1.62)	−4.47	***	.20
$EVI_{pre\text{-}cyclone}$	0.03 (0.01)	4.35	***	.20	4.07 (1.85)	2.20	*	.06
Mean AGB	−0.04 (0.01)	−4.11	***	.18	−9.85 (2.48)	−3.98	***	.17
Frequency	−0.02 (0.01)	−2.35	*	.07	−3.97 (1.84)	−2.16	*	.06
Mean maximum height	0.03 (0.01)	2.64	*	.08	5.81 (2.36)	2.46	*	.07
Annual temperature range	0.01 (0.01)	2.14	*	.06	2.68 (1.57)	1.71		.04
Summary statistics	$n = 86$; df = 78; $F = 13.61$; $p < .01$; AIC = −485.5461; mult. $r^2 = .5499$; adj. $r^2 = .5095$				$n = 86$; df = 78; $F = 12.16$; $p < .01$; AIC = 463.1602; mult. $r^2 = .5219$; adj. $r^2 = .4789$			
NDII								
Intercept	0.10 (0.01)	9.87	***	–	22.87 (2.30)	9.93	***	–
Distance	−0.05 (0.01)	−4.51	***	.20	−10.70 (2.45)	−4.37	***	.19
Wind speed	0.04 (0.01)	3.34	**	.12	8.39 (2.50)	3.36	**	.12
Frequency	−0.02 (0.01)	−1.51		.03	−4.09 (2.55)	−1.60		.03
Mean AGB	−0.05 (0.02)	−2.70	**	.08	−9.63 (3.73)	−2.58	*	.08
$NDII_{pre\text{-}cyclone}$					−5.55 (2.36)	−2.35	*	.07
Mean maximum height	0.03 (0.02)	2.08	*	.05	6.84 (3.53)	1.94		.05
Summary statistics	$n = 86$; df = 80; $F = 13.51$; $p < .01$; AIC = −394.9849; mult. $r^2 = .4578$; adj. $r^2 = .4239$				$n = 86$; df = 79; $F = 13.28$; $p < .01$; AIC = 533.2275; mult. $r^2 = .5021$; adj. $r^2 = .4643$			

Note: Multiple r^2 (mult. r^2), adjusted r^2 (adj. r^2) and the Akaike information criterion (AIC) are indicated for each model. Detailed model selections and variance inflation factor (VIF) scores are shown in the Supporting Information (Tables S4 and S5). The Supporting Information (Table S6) describes multiple linear regression results based on untransformed ΔVIs.

Abbreviation: AGB, aboveground biomass.

*$p < .05$; **$p < .01$; ***$p < .001$.

index reduction; Table 1). Moreover, we report that distance was the most important factor explaining the variation of cyclone-induced canopy damage (Figure 3), probably because a shorter distance to the cyclone path implies higher wind speed and a longer exposure time of the mangrove forest canopy to the winds of the cyclone. A site-based study from the Fushan Experimental Forest of northern Taiwan, which experiences roughly one cyclone of at least category 3 every 2 years, also found that cyclone proximity is the chief factor determining remotely sensed cyclone-induced canopy loss of tropical broadleaf forest (Peereman et al., 2020). Given that the effects of cyclones are likely to be consistent across much of the zone of cyclone influence (Ibanez et al., 2018), distance is likely to be the principal factor in modulating cyclone effects on forests across multiple scales, from the local to global scale.

Wind speed is another main factor in determining the severity of cyclone damage. Positive relationships between damage severity and cyclone wind speed have been reported for mangroves in the Caribbean and Gulf of Mexico region (Imbert, 2018; Taillie et al., 2020). Our results indicate that the positive relationship between the magnitude of damage and wind speed holds globally. The positive relationship between wind speed and the damage severity indicates that, even among major cyclones, greater wind speed still results in greater mangrove canopy loss. However, we detected little to no damage caused by cyclones of up to category 2, which might be the product of the limited sensitivity of the VIs to slight canopy damage or might reflect a wind speed threshold for leaf loss in mangroves (Zhang et al., 2016). The projected increases in the intensity of cyclones and the frequency

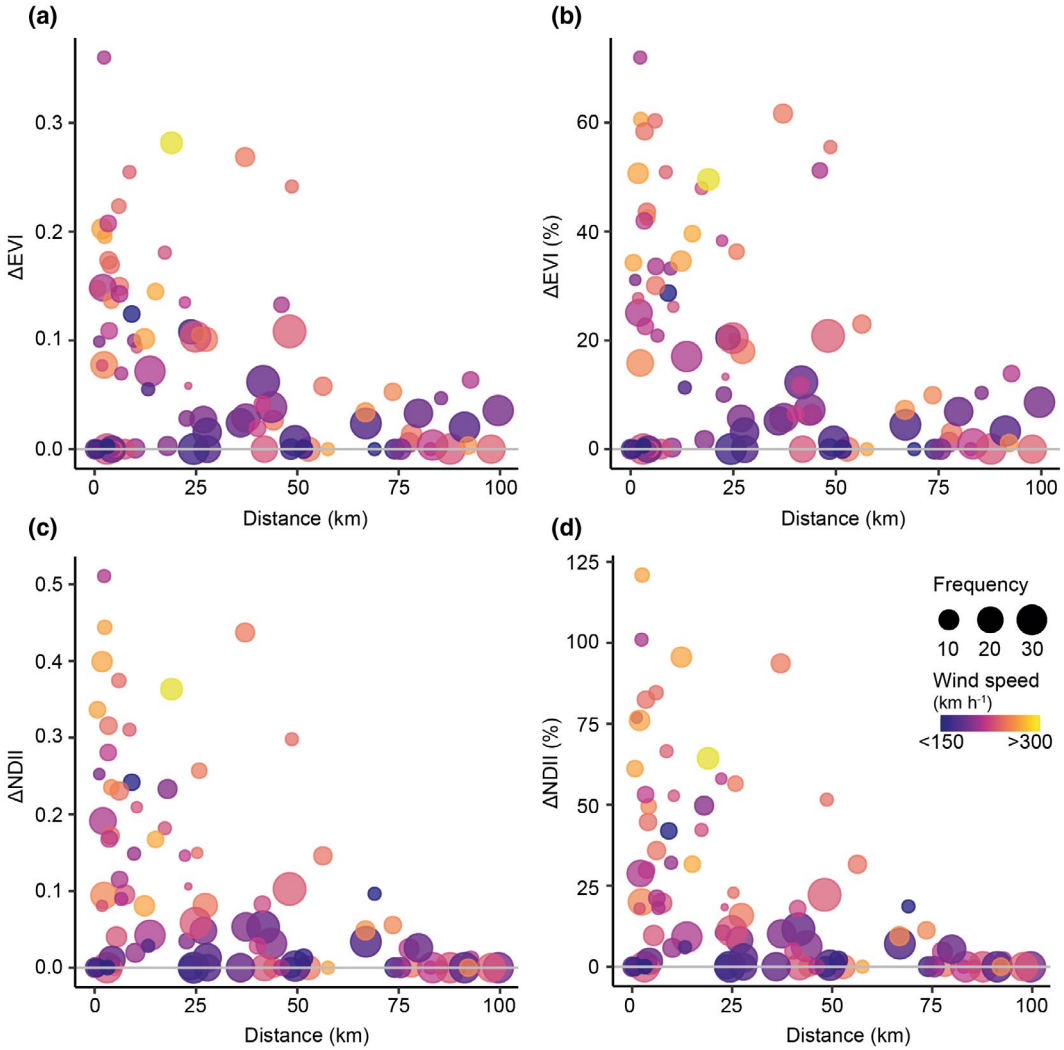

FIGURE 2 The absolute and relative change of (a,b) enhanced vegetation index (EVI) and (c,d) normalized difference infrared index (NDII) in relationship to the minimum distance between cyclone path and site centroid, cyclone maximum sustained wind speed and cyclone frequency ($n = 86$)

of the most intense cyclones (Kossin et al., 2020) are therefore likely to cause greater vegetation loss in mangrove forests than has been observed previously. Moreover, with the projected poleward shift in the latitudinal distribution of cyclones and their migration closer to coastlines (Altman et al., 2018; Wang & Toumi, 2021), it is likely that in the coming decades, mangrove areas of Australia, India and South-eastern Africa, which have not experienced cyclone disturbances historically, might experience them. Such changes potentially have major implications for the global carbon cycle, including reduced uptake and sequestration, because mangrove forests play a disproportionate role in these processes (Barr et al., 2012).

A remote sensing-based study of hurricane disturbances in the Caribbean indicated that the recent history of category 1 and 2 hurricanes significantly explained the variation in damage across mangrove forests (Taillie et al., 2020). Mangroves that had been disturbed recently by hurricanes also displayed less damage after the eventful 2017 hurricane season, although the analysis by Taillie et al. (2020) included few major cyclone events, which limits the interpretation of this finding. Being based on a large number of cyclones spread across all cyclone basins, our study clearly shows a positive relationship between cyclone frequency and the resistance of mangrove canopy loss to cyclone disturbance at the global scale. Smaller reductions in EVI for mangroves experiencing more frequent cyclones indicate that mangrove canopies in sites subjected to more frequent cyclones are less vulnerable (i.e., more resistant) to cyclone disturbances (Table 1). Although we cannot discern the type of canopy damage incurred from cyclone events based on the vegetation index values analysed, most detected damage was probably caused by the physical forces of cyclone disturbance (i.e., wind, rainfall and waves) rather than by secondary environmental changes (e.g., change in salinity, warming) associated with the cyclones, given that the post-disturbance Landsat scenes are obtained within 1 month after disturbance. It is likely that slight canopy damage,

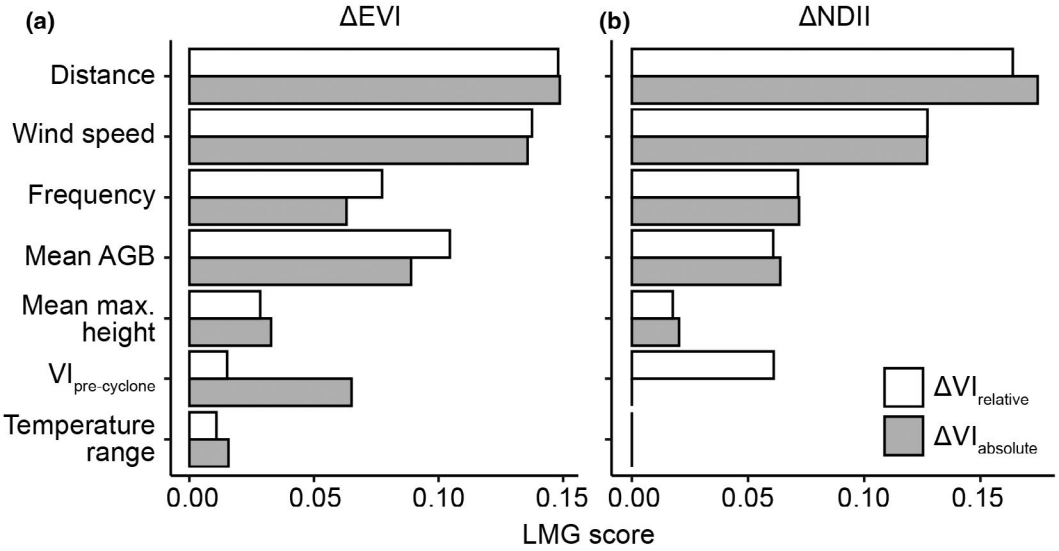

FIGURE 3 The contribution of predictors to multiple linear regression models of the absolute ($\Delta VI_{absolute}$; grey) and relative ($\Delta VI_{relative}$; white) changes in (a) enhanced vegetation index (EVI) and (b) normalized difference infrared index (ΔNDII) caused by cyclones. The Lindeman, Meranda and Gold (LMG) scores are calculated through variance decomposition. The LMG scores indicate the portion of the multiple r^2 of the model that is explained by each predictor; hence, predictors with larger LMG values have a greater contribution to model fits. In (b), predictors without an LMG score were not included in the final linear models after model selection (Table 1). AGB = aboveground biomass; VI = vegetation index

TABLE 2 Linear regression models, with means (*SE*) of coefficients and their *t*-statistics for the time to recovery of enhanced vegetation index (EVI) and the normalized difference infrared index (NDII) following cyclone passages in relationship to variables selected through model selection based on the Akaike information criterion

Predictor	Coefficient (*SE*)	*t*	*p*-value	Partial r^2	LMG
EVI recovery					
Intercept	1.38 (0.36)	3.79	***	–	–
$EVI_{pre\text{-}cyclone}$	0.56 (0.32)	1.73		.11	.02
$\Delta EVI_{relative}$	1.62 (0.36)	4.47	***	.44	.37
Mean AGB	−0.60 (0.41)	−1.46		.08	.01
Annual precipitation	0.46 (0.27)	1.71		.10	.03
Precipitation seasonality	0.61 (0.31)	1.98		.14	.08
Summary statistics	$n = 31$; df = 25; $F = 5.215$; $p < .01$; AIC = 29.54878; mult. $r^2 = .5105$; adj. $r^2 = .4126$				
NDII recovery					
Intercept	1.76 (0.25)	6.89	***		
$\Delta NDII_{absolute}$	1.38 (0.25)	5.61	***	.50	.49
Summary statistics	$n = 34$; df = 32; $F = 31.51$; $p < .01$; AIC = 22.35097; mult. $r^2 = .4961$; adj. $r^2 = .480$				

Note: Multiple r^2 (mult. r^2), adjusted r^2 (adj. r^2) and the Akaike information criterion (AIC) are indicated for each model. The contribution of each predictor is obtained with the Lindeman, Merenda and Gold (LMG) variance decomposition method: r^2 is partitioned among predictors; hence, the sum of LMG equals the model r^2, and larger LMG statistics have greater explanatory power.

***$p < .001$.

such as minor defoliation, might have occurred at most sites, because increased leaf litterfall is commonly reported in mangroves following cyclones (Doyle et al., 1995; Roth, 1992), which increases canopy resistance to high winds by decreasing wind drag (Lin et al., 2020). Severe damage (e.g., large branch fall, bole snapping and tree fall) might have taken place mainly in stands less often disturbed by cyclones because they experienced greater drops in EVI, a metric related to canopy biomass (Huete et al., 1997). Low cyclone-induced tree mortality in ecosystems experiencing frequent cyclone disturbance has been reported in northern Taiwan, in which multiple

category 3 typhoons in a season caused < 2% tree mortality (Lin et al., 2011). This is in stark contrast to the severity of damage observed in sites experiencing lower cyclone frequencies. Indeed, in the Luquillo Experimental Forest of Puerto Rico, 9% of the trees were uprooted and 11% bole-snapped after category 3 Hurricane Hugo (1989), whereas the category 3 1938 hurricane caused 25%–75% tree mortality for 70% of forests of the north-eastern USA (Lin et al., 2011; Mabry et al., 1998).

The mechanisms leading to the high resistance of frequently disturbed mangroves could be explained by more compact canopy structures in areas with frequent cyclones. Wind disturbances trim the upper canopy and prevent individual trees from emerging from the forest canopy (Chi et al., 2015; Doyle et al., 1995; Roth, 1992; Smith et al., 1994). Hence, regular cyclones lead to shorter forests with less vertical canopy surface exposed to wind gusts (Lin et al., 2011, 2020). Shorter forests have higher resistance to canopy loss from cyclones, as indicated by our models (decreasing magnitude of damage for shorter canopy; Table 1) and in several studies (Doyle et al., 1995; Hall et al., 2020; Smith et al., 1994), although the relationship might not be universal in tropical forests (de Gouvenain & Silander, 2003). Indeed, the relationship between cyclone frequency and forest structure appears to be complex (de Gouvenain & Silander, 2003). Unlike the results of Simard et al. (2019a), we did not detect a significant relationship between cyclone frequency and maximum canopy height. However, another possibility for the lack of a significant relationship in our study is that we used a much smaller dataset than study by Simard et al. (2019a), which spanned the entire geographical distribution of mangrove forests, whereas ours was limited to mangrove areas affected by cyclone disturbance. Thus, the increasing frequency of intense cyclones (Kossin et al., 2020) might lead to overall shorter mangrove canopies globally, in areas currently affected and those that might be affected in the near future (Altman et al., 2018; Doyle & Girod, 1997; Wang & Toumi, 2021).

Forest structural attributes other than canopy height modulate the susceptibility of forest stands to cyclone-induced canopy damage. Following Hurricane Katrina, Wang and Xu (2009) reported reduced damage in forests with greater vegetation cover and stand density, both of which contribute to higher AGB. Moreover, Rovai et al. (2021) indicated that cyclone frequency does not drive the global variation in mangrove AGB, and our study suggests that this observation holds within geographical limits of cyclone influence ($p < .05$). Although mangrove basal area and canopy height contribute positively to AGB (Rovai et al., 2021), our study showed that damage decreased when AGB increased and when the canopy was shorter. Moreover, we found that the AGB contributed three times more than mean maximum canopy height in explaining variation in vegetation index change because of cyclone disturbance (12–20% vs. 4–6%; Figure 3). With the adjusted $r^2 \leq .51$ for the regression models of ΔVIs (Table 1), it is likely that other forest attributes (e.g., stand density, d.b.h. and species identity) that could not be included in our models could be important determinants of cyclone-induced vegetation loss. Nevertheless, these findings suggest that global resistance of mangroves to cyclones might be mainly the product of high AGB rather than shorter canopy, perhaps through a contribution of tree stem density and tree size (i.e., d.b.h.). Indeed, less dense stands can show greater openness, hence greater wind penetration and therefore higher wind-induced damage (Kim et al., 2020). In turn, disturbances can return forests to an earlier successional stage, which is characterized by higher tree densities, shorter tree heights and overall higher resistance to subsequent cyclone disturbance (Flynn et al., 2010).

4.2 | Rates of mangrove canopy recovery are consistent globally

Understanding forest recovery dynamics following cyclone disturbance is important for modelling mangrove forest carbon fluxes and for evaluating thresholds of resistance and resilience to disturbance in mangrove forests (Barr et al., 2012; Lagomasino et al., 2021). One might hypothesize that mangrove stands that experience more frequent defoliating cyclones might recover canopies faster than those that experience less frequent defoliation. Instead, we found that mangroves subject to frequent cyclone disturbance did not recover faster than those experiencing less frequent cyclone disturbance because the magnitude of cyclone-induced damage was the only significant and major predictor of time to recovery of EVI and NDII (Table 2). Mangrove forests sustaining more severe VI reductions (i.e., canopy loss) logically take a longer time to recover (e.g., because of damage to branches; Radabaugh et al., 2020). Yet, it is surprising that climatic variables (e.g., rainfall and temperature) played little role, given that periods of low rainfall are known to depress mangrove tree growth and recovery (Gang et al., 2020). Nevertheless, other vegetation-related factors not included in our linear models, such as species composition, might play a role in explaining canopy recovery rates (Duke, 2001; Imbert, 2018; Radabaugh et al., 2020), and the lack of inclusion of these variables probably contributes to the marginal predictive power of the linear models (adjusted $r^2 \leq .48$; Table 2).

Similar canopy recovery times, coupled with the negative relationship between cyclone frequency and cyclone-induced vegetation loss, suggest that mangrove forest canopies with more frequent cyclone disturbances are less damaged (i.e., more resistant) but recover at similar rates, with the main factor that governs recovery time being the magnitude of canopy damage. Hence, globally, variation in mangrove canopy resilience to cyclone disturbance is a function of their resistance (e.g., low vulnerability to cyclone damage in regions experiencing frequent disturbances) and not their ability to recover more quickly following cyclone disturbance. This pattern certainly explains why large mangrove forests are present in the Northwestern Pacific, a region with a high cyclone frequency (Supporting Information Table S1), although the dominant mangrove trees belong to the Rhizophoraceae (Nakasuga, 1979) and can only recover through

propagule production and not grow epicormic shoots (Duke, 2001). Our finding that canopy recovery might be similar across mangroves highlights the risk faced by mangroves in regions where the frequency of intense cyclones is increasing (Kossin et al., 2020; Wang & Toumi, 2021), because these forests might not have time to recover between disturbances if they become more severely disturbed.

Nevertheless, the remote sensing approach taken in the present study to measure canopy damage (i.e., ΔVI) does not translate into precise measurement of types of damage; hence, a similar ΔVI could be observed from defoliation or structural canopy damage (e.g., branch and stem breakage). This variation feeds back to induce variation in canopy recovery time, because VI reduction associated with defoliation is recovered faster than VI reduction associated with branch breakage or tree fall (Radabaugh et al., 2020; Smith et al., 1994).

4.3 | Vegetation indices as a tool for global ecology

Remotely sensed VIs are used widely and increasingly more often in disturbance ecology to monitor canopy dynamics over large areas (Gang et al., 2020; Taillie et al., 2020). The relationship between spectral bands and leaf characteristics makes it possible to track the effect of hurricanes, cold waves and other disturbance drivers of mangroves canopy loss (e.g., Zhang et al., 2016). Zhang et al. (2016) concluded that the NDII was among the most sensitive indices to follow the change of the mangrove canopy. In our study, the magnitude of cyclone-mediated EVI change was related to cyclone frequency, whereas that was not the case for NDII, which suggests that the change in canopy structure is likely to be related to change in biomass (e.g., via defoliation; Huete et al., 1997), but not cyclone-induced change in canopy moisture, to which NDII is sensitive (Cheng et al., 2006). Furthermore, the magnitude of damage increased with pre-cyclone EVI but decreased with pre-cyclone NDII. Hence, we suggest using multiple VIs in the monitoring of forest disturbances because different VIs are likely to track different aspects of the mangrove canopies.

5 | CONCLUSIONS

Using two VIs derived from satellite images and other freely available datasets, we have detected cyclone-induced mangrove forest canopy damage and recovery patterns and their drivers, which scale globally. We confirm the importance of cyclone characteristics, such as wind speed and storm distance, in modulating the effects of cyclones on mangrove canopy loss and recovery across the world. However, we report a novel finding, whereby both greater cyclone frequency and stand AGB reduced the magnitude of cyclone-induced canopy vegetation loss. Additionally, mean mangrove canopy height was positively related to cyclone-induced vegetation losses, suggesting that more mature mangrove stands are potentially more vulnerable to cyclone damage, especially in regions that experience few cyclones. Most importantly, cyclone characteristics do not affect rates of mangrove canopy recovery after cyclone disturbance. We propose that globally, the resilience of mangrove forests to cyclone disturbance (i.e., canopy recovery time) is related to forest resistance (i.e., the vulnerability of a stand to cyclone damage), instead of rates of canopy recovery. These findings imply that as cyclones move closer to unaffected coastal areas, both poleward and more inland, and as they intensify with climate change, they might cause increasing damage to mangrove forests in the coming decades to centuries, especially if changes in cyclone disturbance regimes are coupled with an increase in frequency and severity of other stressors (e.g., drought).

ACKNOWLEDGMENTS

We thank Pei-Jen Lee Shaner for assistance with statistical analysis. We acknowledge the use of Landsat data, which are a NASA product. This research is supported by grants from the Ministry of Science and Technology (MOST 107-2313-B-003-001-MY3).

CONFLICT OF INTEREST

The authors declare that there is no conflict of interest that could be perceived as prejudicing the impartiality of the research reported.

DATA AVAILABILITY STATEMENT

The data supporting the results are all from publically accessible sources. The satellite images are from USGS Earthexplorer website (http://earthexplorer.usgs.gov), the climate data are from the WorldClim v.2 dataset, and the mangrove aboveground biomass and canopy height are from the CMS dataset of global mangrove distribution, aboveground biomass and canopy height in the ORNL Distributed Active Archive Center (https://doi.org/10.3334/ORNLDAAC/1665). Mangrove distribution data are from the Global Distribution of Mangroves (https://doi.org/10.34892/1411-w728) and the Global Mangrove Watch data (GMW) between 1996 and 2016 (https://data.unep-wcmc.org/datasets/45). The sources are all described clearly in the manuscript. In addition, the file names of images used are listed in the Supporting Information (Table S2), meaning that they can be retrieved easily.

ORCID

Jonathan Peereman https://orcid.org/0000-0002-5128-3536
J. Aaron Hogan https://orcid.org/0000-0001-9806-3074
Teng-Chiu Lin https://orcid.org/0000-0003-1088-8771

REFERENCES

Adame, M. F., Zaldívar-Jimenez, A., Teutli, C., Caamal, J. P., Andueza, M. T., López-Adame, H., Cano, R., Hernández-Arana, H. A., Torres-Lara, R., & Herrera-Silveira, J. A. (2013). Drivers of mangrove litterfall within a karstic region affected by frequent hurricanes. *Biotropica*, *45*, 147–154. https://doi.org/10.1111/btp.12000

Allen, J. A., Ewel, K. C., Keeland, B. D., Tara, T., & Smith, T. J. (2000). Downed wood in Micronesian mangrove forests. *Wetlands*, *20*,

169–176. https://doi.org/10.1672/0277-5212(2000)020[0169:DWIMMF]2.0.CO;2

Alongi, D. M. (2015). The impact of climate change on mangrove forests. *Current Climate Change Reports*, *1*, 30–39. https://doi.org/10.1007/s40641-015-0002-x

Altman, J., Ukhvatkina, O. N., Omelko, A. M., Macek, M., Plener, T., Pejcha, V., Cerny, T., Petrik, P., Srutek, M., Song, J.-S., Zhmerenetsky, A. A., Vozmishcheva, A. S., Krestov, P. V., Petrenko, T. Y., Treydte, K., & Dolezal, J. (2018). Poleward migration of the destructive effects of tropical cyclones during the 20th century. *Proceedings of the National Academy of Sciences USA*, *115*, 11543–11548. https://doi.org/10.1073/pnas.1808979115

Barr, J. G., Engel, V., Smith, T. J., & Fuentes, J. D. (2012). Hurricane disturbance and recovery of energy balance, CO_2 fluxes and canopy structure in a mangrove forest of the Florida Everglades. *Agricultural and Forest Meteorology*, *153*, 54–66. https://doi.org/10.1016/j.agrformet.2011.07.022

Branoff, B. L. (2017). Quantifying the influence of urban land use on mangrove biology and ecology: A meta-analysis. *Global Ecology and Biogeography*, *26*, 1339–1356. https://doi.org/10.1111/geb.12638

Bunting, P., Rosenqvist, A., Lucas, R., Rebelo, L.-M., Hilarides, L., Thomas, N., Hardy, A., Itoh, T., Shimada, M., & Finlayson, C. (2018). The global mangrove watch—A new 2010 global baseline of mangrove extent. *Remote Sensing*, *10*, 1669. https://doi.org/10.3390/rs10101669

Cameron, C., Kennedy, B., Tuiwawa, S., Goldwater, N., Soapi, K., & Lovelock, C. E. (2021). High variance in community structure and ecosystem carbon stocks of Fijian mangroves driven by differences in geomorphology and climate. *Environmental Research*, *192*, 110213. https://doi.org/10.1016/j.envres.2020.110213

Castañeda-Moya, E., Rivera-Monroy, V. H., Chambers, R. M., Zhao, X., Lamb-Wotton, L., Gorsky, A., Gaiser, E. E., Troxler, T. G., Kominoski, J. S., & Hiatt, M. (2020). Hurricanes fertilize mangrove forests in the Gulf of Mexico (Florida Everglades, USA). *Proceedings of the National Academy of Sciences USA*, *117*, 4831–4841. https://doi.org/10.1073/pnas.1908597117

Castañeda-Moya, E., Twilley, R. R., & Rivera-Monroy, V. H. (2013). Allocation of biomass and net primary productivity of mangrove forests along environmental gradients in the Florida Coastal Everglades, USA. *Forest Ecology and Management*, *307*, 226–241. https://doi.org/10.1016/j.foreco.2013.07.011

Cheng, Y.-B., Zarco-Tejada, P. J., Riaño, D., Rueda, C. A., & Ustin, S. L. (2006). Estimating vegetation water content with hyperspectral data for different canopy scenarios: Relationships between AVIRIS and MODIS indexes. *Remote Sensing of Environment*, *105*, 354–366. https://doi.org/10.1016/j.rse.2006.07.005

Chi, C.-H., McEwan, R. W., Chang, C.-T., Zheng, C., Yang, Z., Chiang, J.-M., & Lin, T.-C. (2015). Typhoon disturbance mediates elevational patterns of forest structure, but not species diversity, in humid monsoon Asia. *Ecosystems*, *18*, 1410–1423. https://doi.org/10.1007/s10021-015-9908-3

de Gouvenain, R. C., & Silander, J. A. (2003). Do tropical storm regimes influence the structure of tropical lowland rain forests? *Biotropica*, *35*, 166–180. https://doi.org/10.1111/j.1744-7429.2003.tb00276.x

Din, N., Saenger, P., Jules, P. R., Siegfried, D. D., & Basco, F. (2008). Logging activities in mangrove forests: A case study of Douala Cameroon. *African Journal of Environmental Science and Technology*, *2*, 22–30.

Doyle, T. W., & Girod, G. F. (1997). The frequency and intensity of Atlantic hurricanes and their influence on the structure of South Florida mangrove communities. In H. F. Diaz, & R. S. Pulwarty (Eds.), *Hurricanes: Climate and socioeconomic impacts* (pp. 109–120). Springer.

Doyle, T. W., Smith, T. J., & Robblee, M. B. (1995). Wind damage effects of Hurricane Andrew on mangrove communities along the southwest coast of Florida, USA [Special issue]. *Journal of Coastal Research*, (21), 159–168.

Duke, N. C. (2001). Gap creation and regenerative processes driving diversity and structure of mangrove ecosystems. *Wetlands Ecology and Management*, *9*, 267–279. https://doi.org/10.1023/A:1011121109886

Ferwerda, J. G., Ketner, P., & McGuinness, K. A. (2007). Differences in regeneration between hurricane damaged and clear-cut mangrove stands 25 years after clearing. *Hydrobiologia*, *591*, 35–45. https://doi.org/10.1007/s10750-007-0782-7

Fick, S. E., & Hijmans, R. J. (2017). WorldClim 2: New 1-km spatial resolution climate surfaces for global land areas. *International Journal of Climatology*, *37*, 4302–4315. https://doi.org/10.1002/joc.5086

Flynn, D. F. B., Uriarte, M., Crk, T., Pascarella, J. B., Zimmerman, J. K., Aide, T. M., & Ortiz, M. A. C. (2010). Hurricane disturbance alters secondary forest recovery in Puerto Rico. *Biotropica*, *42*, 149–157. https://doi.org/10.1111/j.1744-7429.2009.00581

Gang, C., Pan, S., Tian, H., Wang, Z., Xu, R., Bian, Z., Pan, N., Yao, Y., & Shi, H. (2020). Satellite observations of forest resilience to hurricanes along the northern Gulf of Mexico. *Forest Ecology and Management*, *472*, 118243. https://doi.org/10.1016/j.foreco.2020.118243

Giri, C., Ochieng, E., Tieszen, L. L., Zhu, Z., Singh, A., Loveland, T., Masek, J., & Duke, N. (2011). Status and distribution of mangrove forests of the world using earth observation satellite data. *Global Ecology and Biogeography*, *20*, 154–159. https://doi.org/10.1111/j.1466-8238.2010.00584.x

Gough, C. M., Atkins, J. W., Bond-Lamberty, B., Agee, E. A., Dorheim, K. R., Fahey, R. T., Grigri, M. S., Haber, L. T., Mathes, K. C., Pennington, S. C., Shiklomanov, A. N., & Tallant, J. M. (2021). Forest structural complexity and biomass predict first-year carbon cycling responses to disturbance. *Ecosystems*, *24*, 699–712. https://doi.org/10.1007/s10021-020-00544-1

Grömping, U. (2006). Relative importance for linear regression in R: The package relaimpo. *Journal of Statistical Software*, *17*(1), 1–27. https://doi.org/10.18637/jss.v017.i01

Hall, J., Muscarella, R., Quebbeman, A., Arellano, G., Thompson, J., Zimmerman, J. K., & Uriarte, M. (2020). Hurricane-induced rainfall is a stronger predictor of tropical forest damage in Puerto Rico than maximum wind speeds. *Scientific Reports*, *10*, 4318. https://doi.org/10.1038/s41598-020-61164-2

Hardisky, M. A., Klemas, V., & Smart, R. M. (1983). The influence of soil salinity, growth form, and leaf moisture on the spectral reflectance of *Spartina alterniflora* canopies. *Photogrammetric Engineering and Remote Sensing*, *49*, 77–83.

Herberich, E., Sikorski, J., & Hothorn, T. (2010). A robust procedure for comparing multiple means under heteroscedasticity in unbalanced designs. *PLoS One*, *5*, e9788. https://doi.org/10.1371/journal.pone.0009788

Hijmans, R. J. (2019). *raster: Geographic data analysis and modeling (Version 2.9-23)*. Retrieved from https://CRAN.R-project.org/package=raster

Hogan, J. A., Zimmerman, J. K., Thompson, J., Uriarte, M., Swenson, N. G., Condit, R., & Davies, S. J. (2018). The frequency of cyclonic wind storms shapes tropical forest dynamism and functional

trait dispersion. *Forests*, *9*, 404. https://doi.org/10.3390/f9070404

Holling, C. S. (1973). Resilience and stability of ecological systems. *Annual Review of Ecology and Systematics*, *4*, 1–23. https://doi.org/10.1146/annurev.es.04.110173.000245

Hothorn, T., Bretz, F., & Westfall, P. (2008). Simultaneous inference in general parametric models. *Biometrical Journal*, *50*, 346–363. https://doi.org/10.1002/bimj.200810425

Huete, A. R., Didan, K., Miura, T., Rodriguez, E. P., Gao, X., & Ferreira, L. G. (2002). Overview of the radiometric and biophysical performance of the MODIS vegetation indices. *Remote Sensing of Environment*, *83*, 195–213. https://doi.org/10.1016/s0034-4257(02)00096-2

Huete, A. R., Liu, H., & van Leeuwen, W. J. (1997). *The use of vegetation indices in forested regions: Issues of linearity and saturation*. Paper presented to the 1997 IEEE International Geoscience and Remote Sensing Symposium Proceedings. Remote Sensing—A Scientific Vision for Sustainable Development, Singapore.

Ibanez, T., Keppel, G., Menkes, C., Gillespie, T. W., Lengaigne, M., Mangeas, M., Rivas-Torres, G., & Birnbaum, P. (2018). Globally consistent impact of tropical cyclones on the structure of tropical and subtropical forests. *Journal of Ecology*, *107*, 279–292. https://doi.org/10.1111/1365-2745.13039

Imbert, D. (2018). Hurricane disturbance and forest dynamics in east Caribbean mangroves. *Ecosphere*, *9*, e02231. https://doi.org/10.1002/ecs2.2231

Kauffman, J. B., & Cole, T. G. (2010). Micronesian mangrove forest structure and tree responses to a severe typhoon. *Wetlands*, *30*, 1077–1084. https://doi.org/10.1007/s13157-010-0114-y

Kim, D., Millington, A. C., & Lafon, C. W. (2020). Disturbance after disturbance: Combined effects of two successive hurricanes on forest community structure. *Annals of the American Association of Geographers*, *110*, 571–585. https://doi.org/10.1080/24694452.2019.1654844

Knapp, K. R., Diamond, H. J., Kossin, J. P., Kruk, M. C., & Schreck, C. J. (2018). *International best track archive for climate stewardship (IBTrACS) project, Version 4. [IBTrACS.ALL.list.v04r00] NOAA National Centers for Environmental Information*. https://doi.org/10.25921/82ty-9e16

Knapp, K. R., Kruk, M. C., Levinson, D. H., Diamond, H. J., & Neumann, C. J. (2010). The international best track archive for climate stewardship (IBTrACS): Unifying tropical cyclone best track data. *Bulletin of the American Meteorological Society*, *91*, 363–376. https://doi.org/10.1175/2009BAMS2755.1

Kossin, J. P., Knapp, K. R., Olander, T. L., & Velden, C. S. (2020). Global increase in major tropical cyclone exceedance probability over the past four decades. *Proceedings of the National Academy of Sciences USA*, *117*, 11975–11980. https://doi.org/10.1073/pnas.1920849117

Kosugi, R., Shibuya, M., & Ishibashi, S. (2016). Sixty-year post-windthrow study of stand dynamics in two natural forests differing in pre-disturbance composition. *Ecosphere*, *7*, e01571. https://doi.org/10.1002/ecs2.1571

Krauss, K. W., & Osland, M. J. (2020). Tropical cyclones and the organization of mangrove forests: A review. *Annals of Botany*, *125*, 213–234. https://doi.org/10.1093/aob/mcz161

Lagomasino, D., Fatoyinbo, T., Castañeda-Moya, E., Cook, B. D., Montesano, P. M., Neigh, C. S. R., & Morton, D. C. (2021). Storm surge and ponding explain mangrove dieback in southwest Florida following Hurricane Irma. *Nature Communications*, *12*, 4003. https://doi.org/10.1038/s41467-021-24253-y

Lin, K.-C., Hamburg, S. P., Tang, S.-L., Hsia, Y.-J., & Lin, T.-C. (2003). Typhoon effects on litterfall in a subtropical forest. *Canadian Journal of Forest Research*, *33*, 2184–2192. https://doi.org/10.1139/x03-154

Lin, T.-C., Hamburg, S. P., Lin, K.-C., Wang, L.-J., Chang, C.-T., Hsia, Y.-J., & Liu, C.-P. (2011). Typhoon disturbance and forest dynamics: Lessons from a Northwest Pacific subtropical forest. *Ecosystems*, *14*, 127–143. https://doi.org/10.1007/s10021-010-9399-1

Lin, T.-C., Hogan, J. A., & Chang, C.-T. (2020). Tropical cyclone ecology: A scale-link perspective. *Trends in Ecology and Evolution*, *7*, 594–604. https://doi.org/10.1016/j.tree.2020.02.012

Lindeman, R. H., Merenda, P. F., & Gold, R. Z. (1980). *Introduction to bivariate and multivariate analysis*. Scott.

Lovelock, C. E., Cahoon, D. R., Friess, D. A., Guntenspergen, G. R., Krauss, K. W., Reef, R., & Triet, T. (2015). The vulnerability of Indo-Pacific mangrove forests to sea-level rise. *Nature*, *526*, 559–563. https://doi.org/10.1038/nature15538

Mabry, C. M., Hamburg, S. P., Lin, T.-C., Horng, F.-W., King, H.-B., & Hsia, Y.-J. (1998). Typhoon disturbance and stand-level damage patterns at a subtropical forest in Taiwan. *Biotropica*, *30*, 238–250. https://doi.org/10.1111/j.1744-7429.1998.tb00058.x

Nakasuga, T. (1979). Analysis of the mangrove stand. *The Science Bulletin of the Faculty of Agriculture. University of the Ryukyus, Okinawa*, *26*, 413–519.

Pastor-Guzman, J., Dash, J., & Atkinson, P. M. (2018). Remote sensing of mangrove forest phenology and its environmental drivers. *Remote Sensing of Environment*, *205*, 71–84. https://doi.org/10.1016/j.rse.2017.11.009

Peereman, J., Hogan, J. A., & Lin, T.-C. (2020). Assessing typhoon-induced canopy damage using vegetation indices in the Fushan Experimental Forest, Taiwan. *Remote Sensing*, *12*, 1654. https://doi.org/10.3390/rs12101654

Peneva-Reed, E. I., Krauss, K. W., Bullock, E. L., Zhu, Z., Woltz, V. L., Drexler, J. Z., & Stehman, S. V. (2020). Carbon stock losses and recovery observed for a mangrove ecosystem following a major hurricane in Southwest Florida. *Estuarine, Coastal and Shelf Science*, *248*, 106750. https://doi.org/10.1016/j.ecss.2020.106750

R Core Team. (2019). *R: A language and environment for statistical computing*. R Foundation for Statistical Computing. Retrieved from https://www.R-project.org/

Radabaugh, K. R., Moyer, R. P., Chappel, A. R., Dontis, E. E., Russo, C. E., Joyse, K. M., & Khan, N. S. (2020). Mangrove damage, delayed mortality, and early recovery following Hurricane Irma at two landfall sites in Southwest Florida, USA. *Estuaries and Coasts*, *43*, 1104–1118. https://doi.org/10.1007/s12237-019-00564-8

Roth, L. C. (1992). Hurricanes and mangrove regeneration: Effects of Hurricane Joan, October 1988, on the vegetation of Isla del Venado, Bluefields, Nicaragua. *Biotropica*, *24*, 375–384. https://doi.org/10.2307/2388607

Rovai, A. S., Coelho-Jr, C., de Almeida, R., Cunha-Lignon, M., Menghini, R. P., Twilley, R. R., Cintrón-Molero, G., & Schaeffer-Novelli, Y. (2021). Ecosystem-level carbon stocks and sequestration rates in mangroves in the Cananéia-Iguape lagoon estuarine system, southeastern Brazil. *Forest Ecology and Management*, *479*, 118553. https://doi.org/10.1016/j.foreco.2020.118553

Rovai, A. S., Riul, P., Twilley, R. R., Castañeda-Moya, E., Rivera-Monroy, V. H., Williams, A. A., Simard, M., Cifuentes-Jara, M., Lewis, R. R., Crooks, S., Horta, P. A., Schaeffer-Novelli, Y., Cintrón, M., Pozo-Cajas, P., & Pagliosa, P. R. (2016). Scaling mangrove aboveground biomass from site-level to continental-scale. *Global Ecology and Biogeography*, *25*, 286–298. https://doi.org/10.1111/geb.12409

Simard, M., Fatoyinbo, L., Smetanka, C., Rivera-Monroy, V. H., Castañeda-Moya, E., Thomas, N., & Van der Stocken, T. (2019a). Mangrove canopy height globally related to precipitation, temperature and cyclone frequency. *Nature Geoscience*, *12*, 40–45. https://doi.org/10.1038/s41561-018-0279-1

Simard, M., Fatoyinbo, T., Smetanka, C., Rivera-Monroy, V. H., Castaneda-Mova, E., Thomas, N., & Van Der Stocken, T. (2019b). *Global mangrove distribution, aboveground biomass, and canopy height*. Retrieved from https://daac.ornl.gov/cgi-bin/dsviewer.pl?ds_id=1665

Simpson, R. H., & Riehl, H. (1981). *The hurricane and its impact*. Louisiana State University Press.

Smith, T. J. III, Robblee, M. B., Wanless, H. R., & Doyle, T. W. (1994). Mangroves, hurricanes, and lightning strikes: Assessment of Hurricane Andrew suggests an interaction across two differing scales of disturbance. *BioScience*, *44*, 256–262. https://doi.org/10.2307/1312230

Taillie, P. J., Roman-Cuesta, R., Lagomasino, D., Cifuentes-Jara, M., Fatoyinbo, T., Ott, L. E., & Poulter, B. (2020). Widespread mangrove damage resulting from the 2017 Atlantic mega hurricane season. *Environmental Research Letters*, *15*, 064010. https://doi.org/10.1088/1748-9326/ab82cf

UNEP-WCMC, I. (2020). *Protected planet: The World Database on Protected Areas (WDPA)*. Retrieved from https://www.protectedplanet.net/en

Wang, F., & Xu, Y. J. (2009). Hurricane Katrina-induced forest damage in relation to ecological factors at landscape scale. *Environmental Monitoring and Assessment*, *156*, 494–507. https://doi.org/10.1007/s10661-008-0500-6

Wang, S., & Toumi, R. (2021). Recent migration of tropical cyclones toward coasts. *Science*, *371*, 514–517. https://doi.org/10.1126/science.abb9038

Zeileis, A., Köll, S., & Graham, N. (2020). Various versatile variances: An object-oriented implementation of clustered covariances in R. *Journal of Statistical Software*, *95*, 36. https://doi.org/10.18637/jss.v095.i01

Zhang, C., Durgan, S. D., & Lagomasino, D. (2019). Modeling risk of mangroves to tropical cyclones: A case study of Hurricane Irma. *Estuarine, Coastal and Shelf Science*, *224*, 108–116. https://doi.org/10.1016/j.ecss.2019.04.052

Zhang, K., Thapa, B., Ross, M., & Gann, D. (2016). Remote sensing of seasonal changes and disturbances in mangrove forest: A case study from South Florida. *Ecosphere*, *7*, e01366. https://doi.org/10.1002/ecs2.1366

BIOSKETCH

Jonathan Peereman is a postgraduate research associate at National Taiwan Normal University. His research is focused on using remote sensing techniques to inform landscape ecology, specifically the characterization of cyclone disturbance and monitoring of recovery dynamics in tropical forests of Taiwan.

J. Aaron Hogan is a PhD student at Florida International University. He is interested in tropical forest plant and ecosystem ecology. His masters work focused on cyclone disturbance and forest dynamics in Luquillo, Puerto Rico.

Teng-Chiu Lin is an ecosystem ecologist at National Taiwan Normal University. His research is aimed at evaluating ecosystem resilience to tropical cyclone disturbance and anthropogenic stressors, including chronic atmospheric deposition ecosystem dynamics and biogeochemistry of forest ecosystems. Much of his research is conducted at the Fushan Experimental Forest, a long-term ecological research site in Taiwan.

SUPPORTING INFORMATION

Additional Supporting Information may be found in the online version of the article at the publisher's website.

How to cite this article: Peereman, J., Hogan J. A., & Lin T.-C. (2022). Disturbance frequency, intensity and forest structure modulate cyclone-induced changes in mangrove forest canopy cover. *Global Ecology and Biogeography*, 31, 37–50. https://doi.org/10.1111/geb.13407